

Orbit analysis of a geostationary gravitational wave interferometer detector array

Massimo Tinto*

*Jet Propulsion Laboratory,
California Institute of Technology,
Pasadena, CA 91109*

Jose C. N. de Araujo†

*Instituto Nacional de Pesquisas Espaciais,
S. J. Campos, SP, Brazil*

Helio K. Kuga‡

*Instituto Nacional de Pesquisas Espaciais,
S. J. Campos, SP, Brazil*

Márcio E. S. Alves§

*Instituto de Física e Química,
Universidade Federal de Itajubá,
Itajubá, MG, Brazil*

Odylio D. Aguiar¶

*Instituto Nacional de Pesquisas Espaciais,
S. J. Campos, SP, Brazil*

Abstract

We analyze the trajectories of three geostationary satellites forming the GEOstationary GRAvitational Wave Interferometer (GEOGRAWI) [1], a space-based laser interferometer mission aiming to detect and study gravitational radiation in the $(10^{-4} - 10)$ Hz band.

The combined effects of the gravity fields of the Earth, the Sun and the Moon make the three satellites deviate from their nominally stationary, equatorial and equilateral configuration. Since changes in the satellites relative distances and orientations could negatively affect the precision of the laser heterodyne measurements, we have derived the time-dependence of the inter-satellite distances and velocities, the variations of the polar angles made by the constellation's three arms with respect to a chosen reference frame, and the time changes of the triangle's enclosed angles. We find that, during the time between two consecutive station-keeping maneuvers (about two weeks), the relative variations of the inter-satellite distances do not exceed a value of 0.05 percent, while the relative velocities between pairs of satellites remain smaller than about 0.7 m/s. In addition, we find the angles made by the arms of the triangle with the equatorial plane to be periodic functions of time whose amplitudes grow linearly with time; the maximum variations experienced by these angles as well as by those within the triangle remain smaller than 3 arc-minutes, while the East-West angular variations of the three arms remain smaller than about 15 arc-minutes during the two-weeks period. The relatively small variations of these orbit parameters result into a set of system functional and performance requirements that are less stringent than those characterizing an interplanetary mission.

PACS numbers: 95.85.Sz, 04.80.Nn, 95.55.Ym

* massimo.tinto@jpl.nasa.gov

† jcarlos.dearaudo@inpe.br

‡ hkk@dem.inpe.br

§ alvesmes@gmail.com

¶ odylio.aguiar@inpe.br

I. INTRODUCTION

Gravitational waves (GWs), predicted by Einstein’s theory of general relativity, are disturbances of space-time propagating at the speed of light. Because of their extremely small cross-sections, GWs carry information about regions of the Universe that would be otherwise unobtainable through the electromagnetic spectrum. Once detected, GWs will allow us to open a new observational window on the Universe, and perform a unique test of general relativity [2].

Since the first pioneering experiments by Joseph Weber in the early sixties [3], several experimental groups around the world have been attempting to detect GWs. The coming on-line of the Advanced LIGO and Advanced Virgo detectors [4, 5], however, is likely to break this sequence of experimental drawbacks and result into the first detection before the end of this decade.

Contrary to ground-based detectors, which are sensitive to gravitational waves in a band from about a few tens of Hz to a few kilohertz, space-based interferometers are expected to access a much lower frequency region (from a few tenths of millihertz to about a few tens of Hz) where GW signals are expected to be larger in number and characterized by larger amplitudes. The most notable example of a space interferometer, which for several decades has been jointly studied in the United States of America and in Europe, is the Laser Interferometer Space Antenna (LISA) mission [6]. By relying on coherent laser beams exchanged between three remote spacecraft forming a giant (almost) equilateral triangle of arm-length equal to 5×10^6 km, LISA aimed to detect and study cosmic gravitational waves in the $10^{-4} - 1$ Hz band.

Although over the years only a few space-based detector designs have been considered as alternatives to the LISA mission [7–9] starting in 2011 other mission concepts have appeared in the literature [10] in conjunction with the ending of the NASA/ESA partnership for flying LISA. Their goals were to meet (at a lower cost) most (if not all) the LISA scientific objectives (highlighted in the 2010 Astrophysics Decadal Survey *New Worlds, New Horizons (NWNH)* [11]).

GEOGRAWI was one of the alternative concepts to the LISA mission submitted in response to NASA’s Request for Information # NNH11ZDA019L [12]. It entails three spacecraft in geostationary orbit, forming an equilateral triangle of arm-length approximately

equal to 73,000 km. Like LISA, it has three identical spacecraft exchanging coherent laser beams but, by being in a geostationary orbit, it achieves its best sensitivity in a frequency band ($3 \times 10^{-2} - 1$ Hz) [1] that is complementary to those of LISA and ground detectors. The astrophysical sources that GEOGRAWI is expected to observe within its operational frequency band include extra-galactic massive and super-massive black-hole coalescing binaries, the resolved galactic binaries and extra-galactic coalescing binary systems containing white dwarfs and neutron stars, a stochastic background of astrophysical and cosmological origin, and possibly more exotic sources such as cosmic strings. GEOGRAWI will be able to test Einstein’s theory of relativity by comparing the waveforms detected against those predicted by alternative relativistic theories of gravity, and also by measuring the number of independent polarizations of the detected gravitational wave signals [13].

In order to compensate for the gravitational perturbations exerted by the Sun, the Moon, and the gravity field of the Earth (which would result into a long-term orbital drift), a geostationary satellite must perform regular operations of “station-keeping” [14]. This entails firing the onboard thrusters to keep the satellite at its required location. In the case of GEOGRAWI the station-keeping maneuvers performed by its three satellites are particularly important as they offset the excessive variations of the inter-spacecraft relative orientations and velocities and maintain the constellation in a stable configuration. If the spacecraft would be left to drift apart for periods longer than the station-keeping duty cycle, the quality of the laser heterodyne measurements performed by the constellation would degrade, resulting into a degradation of the science objectives of GEOGRAWI [1].

Our paper analyzes the time evolution of the GEOGRAWI constellation during the time between two station-keeping maneuvers, and it is organized as follows. In section II we derive the trajectory of each spacecraft (as a function of time) by numerically solving the Newtonian equations of motion of a “point-particle” in the gravitational potentials of the Earth, the Moon and the Sun. After noticing that the effects of the solar radiation pressure on each spacecraft are not included into the equations of motion because they are compensated for by the spacecraft drag-free system, in section II A we estimate the magnitude of the variations of the inter-spacecraft distances, velocities, and relative angular orientations. We find that, during the time between two consecutive station-keeping maneuvers (about two weeks), the relative variations of the inter-satellite distances do not exceed a value of 0.05 percent, while the relative velocities between pairs of satellites remain smaller than about 0.7 m/s . In

addition, we find the angles made by the arms of the triangle with the equatorial plane to be periodic functions of time whose amplitudes grow linearly with time; the maximum variations experienced by these angles as well as by those within the triangle remain smaller than 3 arc-minutes, while the East-West angular variations of the three arms remain smaller than about 15 arc-minutes during a two-weeks period. These relatively small variations of the orbit parameters result into a set of system performance and functional requirements that are less stringent than those characterizing an interplanetary mission.

II. ORBIT DYNAMICS

GEOGRAWI measures relative frequency changes experienced by coherent laser beams exchanged by its three pairs of spacecraft. As the laser beams are received, they are made to interfere with the outgoing laser light. These heterodyne measurements are each down-converted with the use of an onboard oscillator, then digitized and numerically combined in order to cancel the lasers frequency fluctuations [15]. The spacecraft are made to follow an orbit determined by the gravitational forces on a (spherical) test mass (located onboard each spacecraft) due to the Earth, the Moon and the Sun, and are therefore drag-free. Since the relative distances between spacecraft are not constant, the heterodyne measurements will display a resulting Doppler shifts, which is then removed from the data by using an on-board clock. The magnitude of the frequency fluctuations introduced by the clocks into the heterodyne measurements depends linearly on the noises from the clocks themselves and the inter-spacecraft relative velocities. Space-qualified, state of the art clocks are oven-stabilized crystals characterized by an Allan deviation of $\sigma_A \approx 10^{-13}$ for averaging times of 1 – 1000 s, covering most of the frequency band of interest to GEOGRAWI. The corresponding power spectral density of the relative frequency fluctuations, $S_y(f)$, associated with this “flicker-noise” at the Fourier frequency f is given by the following expression [16]

$$S_y(f) = \frac{\sigma_A^2}{2\ln 2} \frac{\nu_D^2}{\nu_0^2} f^{-1} \text{ Hz}^{-1}, \quad (1)$$

where we have denoted with ν_D the frequency change induced by the Doppler effect on the one-way heterodyne measurement and with ν_0 the nominal laser frequency. Since ν_D is equal to $\nu_D = \nu_0 v/c$, with v being the two spacecraft relative velocity and c the speed of light,

we can rewrite Eq.(1) in the following form

$$S_y(f) = \frac{\sigma_A^2 v^2}{2\ln 2 c^2} f^{-1} \text{ Hz}^{-1}. \quad (2)$$

If we take a spacecraft relative velocity of 0.7 m/s (which we derive in the following subsection II A), a Fourier frequency $f = 10^{-3}$ Hz, and the frequency of the laser to be equal to $\nu_0 = 3.0 \times 10^{14}$ Hz, we find a $S_y(10^{-3}) = 3.9 \times 10^{-41}$ Hz $^{-1}$. To put this number in perspective, in reference [1] we showed that at this frequency the GEOGRAWI noise level goal (determined by our estimate of the remaining noises) was equal to about 3.7×10^{-46} , roughly five orders of magnitude smaller than the above estimated noise due to the clock. Recent developments in the design of space-qualified clocks [17] indicate that oscillators capable of an Allan deviation of a few parts in 10^{-15} or better at 1000 s integration time will be available by the end of this decade. Such a clock performance would still require the implementation of the clock-noise calibration procedure [18] with an inter-spacecraft velocity of 0.7 m/s since the resulting clock noise spectrum would still be about a factor of 10 or so above the GEOGRAWI noises. It should be said, however, that the resulting set of performance requirements levied on the onboard subsystems involved in the clock calibration procedure will be less stringent than those characterizing an interplanetary mission [6] as its inter-spacecraft velocities are approximately 30 times larger than those of GEOGRAWI.

Besides the magnitude of the inter-spacecraft relative velocities, the spacecraft ability of properly pointing to each other is obviously important. In the case of LISA [6], for instance, it was shown that the trajectories of its three spacecraft resulted into a variation of the angles enclosed by the constellation's triangle of about $\pm 1^\circ$. This required the implementation of a mechanical system for articulating the two optical telescopes onboard each spacecraft in such a way to maintain the optical links across the constellation.

In order to address the above questions in the context of GEOGRAWI, in what follows we first integrate the equations of motion for each of the three GEOGRAWI spacecraft. At an arbitrarily chosen starting time $t = 0$, we assume the spacecraft to be at rest with respect to a right-handed, orthogonal coordinate system associated with a reference frame that rotates jointly with the Earth. In it the Z -axis coincides with the Earth's axis of rotation, the X -axis intersects the Greenwich line in the equatorial plane, and the Y axis is orthogonal to it. Under the influence of the Earth, Moon, and Sun gravitational fields, the three spacecraft move from their starting locations corresponding to an equilateral triangle configuration.

Since the Earth is much closer to the spacecraft than the Moon and the Sun, its gravitational potential has to be described mathematically in such a way to reflect the Earth's mass non-spherical and non-symmetrical distribution. This uneven distribution of mass is expressed by the so-called coefficients of spherical harmonics, which enter into the multi-pole expansion of the Earth's gravitational potential (discussed in the appendix). In order to have high accuracy, and because it was also easy to do, our model of the Earth's gravitational potential relied on the EGM2008, which was made to include terms in the multi-pole expansion up to order/degree 2100 [19]. By relying on our numerical integrator [20], we derived the trajectories of the three satellites, i.e. their location and velocity vectors as functions of time. In what follows we provide a description of the kinematic quantities of relevance to GEOGRAWI that we have been able to derive, i.e. the time-dependence of the inter-satellite distances and velocities, and their relative angular orientations.

A. Inter-satellite distances, velocities, and relative orientations

Before describing our estimated relative changes of the three arm-lengths, we should first remind ourselves that the gravity field of the Earth is not invariant under rotation around the Earth's rotation axis because of its non-spherical and non-symmetrical mass distribution. This implies that the variation of the inter-spacecraft distances will depend on the initial longitudinal configuration of the constellation, opening the possibility for the existence of a specific starting longitude of the equilateral triangle minimizing the maximum of the inter-spacecraft velocities. Although there exist a specific value of the longitude of the constellation resulting into a mini-max value of the relative velocities, the resulting reduction in the relative velocities is not significant enough to make it a mission requirement.

In figure (1) we plot the time-dependence of the three inter-spacecraft distances relative to the nominal arm-length of the equilateral triangle at time $t = 0$ (7.3×10^4 km). The plot covers a period of thirty days during which no station-keeping maneuvers have been accounted for. Since these typically happen about once or twice per fortnight, we conclude that during the first, say, fifteen days the maximum relative variations of the three inter-spacecraft distances do not exceed a value of 0.05 percent. Although such small variations of the relative distances, together with the resulting arm-length inequalities, still require GE-OGRAMI to rely on Time-Delay Interferometry (TDI) [15] for canceling the laser frequency

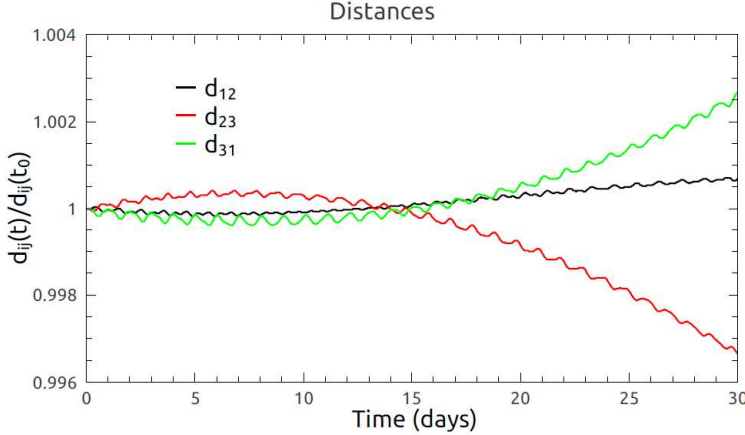


Figure 1. Relative variation of the three inter-spacecraft distances estimated during a period of thirty days. The nominal starting configuration of GEOGRAWI is taken to be an equilateral triangle of arm-length 7.3×10^4 km.

fluctuation, more stable coherent lasers expected to become space-qualified before the end of this decade [21] should allow us to operate GEOGRAWI like a ground-based interferometer.

In figure (2) we now plot the time-dependence of the inter-spacecraft relative velocities, again for a period of thirty days. Note these three time-series are periodic functions of time with period equal to one day and amplitudes that depend on time and do not exceed a maximum value of about 0.7 m/s. Although this is still large enough to require the use of the calibration procedure for canceling the noise from current space-qualified clocks in the GEOGRAWI interferometric measurements, it is still significantly (about a factor of 30) smaller than the values characterizing interplanetary missions [6], making the procedure for its calibration easier to be implemented.

In figure (3) we now plot the variation of the angles enclosed by the triangular constellation. The values shown correspond to the differences between each angle's value at time t and the 60° value at time $t = 0$. During the first two weeks the enclosed angles do not change much, remaining within the ± 3 arc – minute range. To put this number in perspective, in the case of the former LISA mission it was estimated a variation of its enclosed angles of about $\pm 1^\circ$. In order for the LISA spacecraft to track each other it was assessed that each spacecraft had to have an articulation mechanism for varying the angle enclosed by the two onboard optical telescopes. Because of a much smaller variation of its enclosed angles, GEOGRAWI will not need to implement such articulation mechanism.

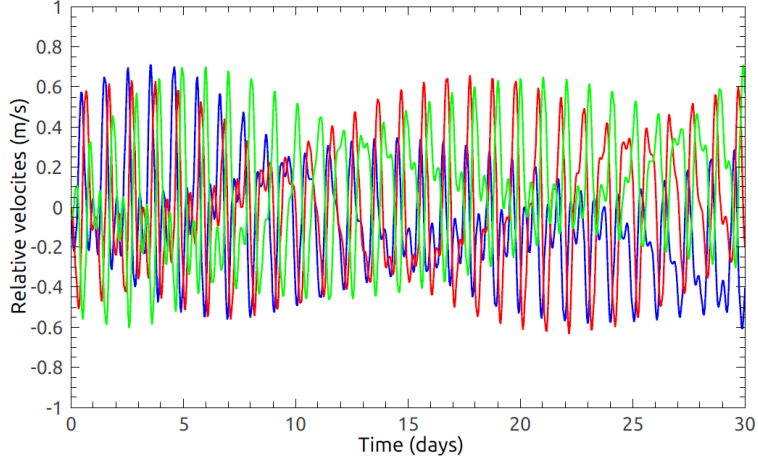


Figure 2. Time-dependence of the inter-spacecraft velocities estimated during a period of thirty days. No station-keeping maneuvers have been accounted for during this time period.

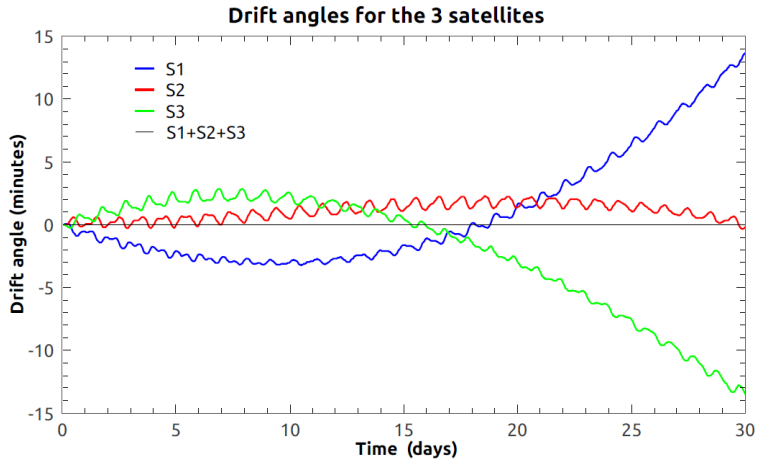


Figure 3. Deviations of the angles enclosed by the constellation with respect to 60^0 , corresponding to the nominal equilateral configuration at time $t = 0$.

To complement the results shown in figure (3) we have derived the variation of the polar angles describing the orientation of each arm of the interferometer. In figure (4) we plot the (i) time-dependence of the three polar angles describing the inclination of the three arms relative to the equatorial plane, and (ii) the inclination of the entire triangle relative to the equatorial plane. The latter is found to be a monotonically growing function of time, changing about 2 arc – minutes during the first fifteen days, while the three polar angles are periodic functions of time and monotonically increasing amplitudes.

Finally in figure (5) we plot the variation of the remaining three polar angles made by the

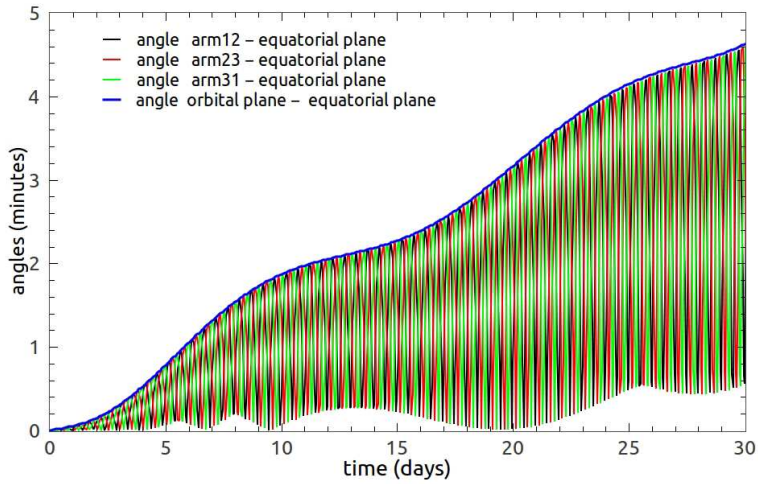


Figure 4. Time-variation of the angles made by the three arms with respect to the equatorial plane. See text for a detailed description.

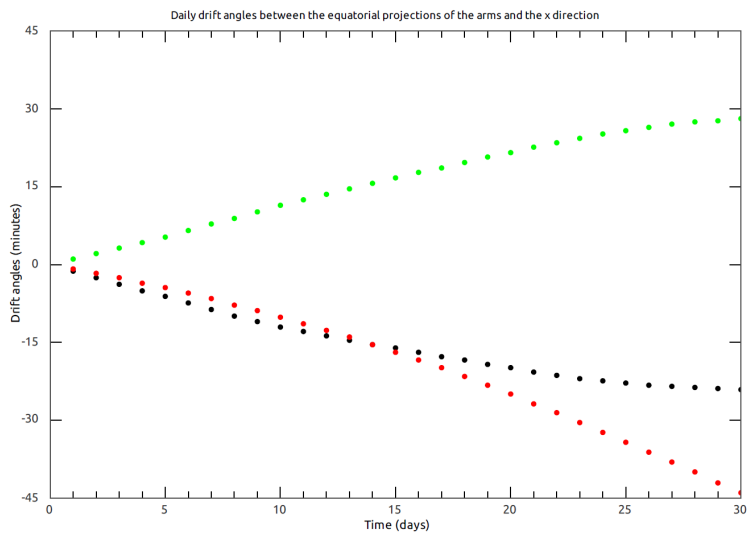


Figure 5. Variation of the angles made by the projections of the three arms over the equatorial plane with an arbitrarily chosen $X-$ axis.

projections of the three arms on the equatorial plane with respect to the $X-$ axis. In this case the variations are larger than those shown in figure (4), but do not exceed a maximum value of 15 arc – minutes during a period of two weeks.

III. CONCLUSIONS

In this article we have analyzed the trajectories of three geostationary satellites forming the constellation of a laser interferometer gravitational wave detector. We have found that, during the time between two consecutive station-keeping maneuvers (about two weeks), the relative variations of the inter-satellite distances do not exceed a value of 0.05 percent, while the relative velocities between pairs of satellites remain smaller than about 0.7 m/s . Since it is likely that future space-qualified clocks will be characterized by a frequency stability that is more than two orders of magnitude better than what currently available, such small relative velocities might imply no need for implementing the clock-noise calibration procedure. This would result into a significant simplification of the hardware architecture that makes the clock-noise calibration procedure possible.

In addition, we found the angles made by the arms of the triangle with the equatorial plane to be periodic functions of time whose amplitudes grow linearly with time; the maximum variations experienced by these angles as well as by those within the triangle remain smaller than 3 arc-minutes, while the East-West angular variations of the three arms remain smaller than about 15 arc-minutes during a two-weeks period. These relatively small variations of the orbit parameters result into a set of system functional and performance requirements that are less stringent than those characterizing an interplanetary mission.

ACKNOWLEDGMENTS

MT acknowledges financial support provided by the Jet Propulsion Laboratory Research & Technology Development program. JCNA thanks FAPESP and CNPq for partial financial support, while MESA acknowledges financial support from FAPEMIG (Grant APQ-00140-12). For MT, this research was performed at the Jet Propulsion Laboratory, California Institute of Technology, under contract with the National Aeronautics and Space Administration.

Appendix A: Orbital Gravitational Effects Computation

A material point (body) subject to attraction by the non-central gravitational field of the Earth suffers disturbances due to non-spherical and non-symmetrical distribution of its

mass. This uneven distribution of mass is expressed by the so-called coefficients of spherical harmonics, and the gravitational potential, V , of a body relative to the Earth is given by the following general multi-poles expansion

$$V = \frac{GM_e}{r} \sum_{n=0}^{\infty} \sum_{m=0}^M \left(\frac{a}{r}\right)^n [\bar{C}_{nm} \cos(m\lambda) + \bar{S}_{nm} \sin(m\lambda)] \bar{P}_{nm}(\sin \Psi), \quad (\text{A1})$$

where G is the universal gravitational constant, M_e is the Earth mass, M is the truncation index, r is the distance to the body from the center of the Earth, a is the Earth equatorial radius, λ is the longitude of the body, Ψ is the geocentric latitude of the body, P_{nm} are the fully normalized Legendre polynomials of order n and degree m , and \bar{C}_{nm} , \bar{S}_{nm} are the fully normalized spherical harmonics coefficients.

Older models of harmonics coefficients did not need analysis or optimization for the numerical computation of the geopotential model. The coefficients were in general of low order and degree. Nowadays the gravitational models easily start from order/degree 360 (like EGM96 model [22]) and go up to more than order/degree 2100 (like EGM2008 (Pavlis et al., 2008, [19])). These computations require the calculation of the Legendre polynomials, which should be recursively evaluated for high order and degree. Herein we used the standard-forward-column implementation proposed by Holmes and Featherstone [23], which is believed to be numerically superior and was described in Kuga and Carrara [20] where its computation performance for Earth orbits was verified.

To implement the algorithm it is convenient to reverse the order of computation of the summation, where the outer loop in m is first computed. Let us rewrite the geopotential summation as:

$$V = \frac{GM}{r} + \frac{GM}{r} \sum_{m=0}^M \left[\cos(m\lambda) \sum_{n=\mu}^M \left(\frac{a}{r}\right)^n \bar{C}_{nm} \bar{P}_{nm}(\Theta) + \sin(m\lambda) \sum_{n=\mu}^M \left(\frac{a}{r}\right)^n \bar{S}_{nm} \bar{P}_{nm}(\Theta) \right], \quad (\text{A2})$$

where $0^\circ < \Theta < 180^\circ$ is now the co-latitude. It is convenient to define the inner terms in equation (A2) as follows:

$$X_{mC} \equiv \sum_{n=\mu}^M \left(\frac{a}{r}\right)^n \bar{C}_{nm} \bar{P}_{nm}(\Theta), \quad X_{mS} \equiv \sum_{n=\mu}^M \left(\frac{a}{r}\right)^n \bar{S}_{nm} \bar{P}_{nm}(\Theta), \quad (\text{A3})$$

$$\Omega_m \equiv \cos(m\lambda)X_{mC} + \sin(m\lambda)X_{mS} , \quad (\text{A4})$$

where μ is an integer that depends on m . By now substituting Eqs. (A3, A4) into Eq. (A2) we finally get

$$V = \frac{GM}{r} + \frac{GM}{r} \sum_{m=0}^M \Omega_m. \quad (\text{A5})$$

The above more compact expression for the potential V allows us to quickly derive the expression of its gradient, which is needed for solving the body's equation of motion. We first evaluate the gradients of the potential with respect to the spherical coordinates λ , Θ , and r . The gradient with respect to λ may be computed by using the following expression

$$V_\lambda \equiv \frac{\partial V}{\partial \lambda} = -\frac{GM}{r} \sum_{m=0}^M m [\sin(m\lambda)X_{mC} - \cos(m\lambda)X_{mS}] , \quad (\text{A6})$$

with X_{mC} and X_{mS} given by equation A3. The computation of the gradients with respect to Θ and r require instead the expressions of the first derivative of the Legendre polynomial, \bar{P}^1 :

$$X_{mC}^\theta \equiv \sum_{n=m}^M \left(\frac{a}{r}\right)^n \bar{C}_{nm} \bar{P}_{nm}^1(\Theta), \quad X_{mS}^\theta \equiv \sum_{n=m}^M \left(\frac{a}{r}\right)^n \bar{S}_{nm} \bar{P}_{nm}^1(\Theta) \quad (\text{A7})$$

$$V_\theta \equiv \frac{\partial V}{\partial \theta} = \frac{GM}{r} \sum_{m=0}^M [\cos(m\lambda)X_{mC}^\theta + \sin(m\lambda)X_{mS}^\theta] , \quad (\text{A8})$$

$$X_{mC}^r \equiv \sum_{n=m}^M \left(\frac{a}{r}\right)^n (n+1) \bar{C}_{nm} \bar{P}_{nm}(\Theta), \quad X_{mS}^r \equiv \sum_{n=m}^M \left(\frac{a}{r}\right)^n (n+1) \bar{S}_{nm} \bar{P}_{nm}(\Theta) , \quad (\text{A9})$$

$$V_r \equiv \frac{\partial V}{\partial r} = -\frac{GM}{r^2} \left\{ 1 + \sum_{m=0}^M [\cos(m\lambda)X_{mC}^r + \sin(m\lambda)X_{mS}^r] \right\} . \quad (\text{A10})$$

The recursion expressions for the Legendre polynomials and their derivatives are given in Kuga and Carrara [20]. Finally, the transformation from spherical to Cartesian coordinates takes into account the partial derivatives that relate them and it is given by the following formulas:

$$\begin{aligned}
\ddot{x} &= u V_r \cos \lambda - \frac{t}{r} V_\theta \cos \lambda - V_\lambda \frac{\sin \lambda}{u r} \\
\ddot{y} &= u V_r \sin \lambda - \frac{t}{r} V_\theta \sin \lambda + V_\lambda \frac{\cos \lambda}{u r} \\
\ddot{z} &= t V_r + \frac{u}{r} V_\theta
\end{aligned} \tag{A11}$$

with $t = \cos(\theta)$ and $u = \sin(\theta)$. The implemented codes [20] were tested up to order 2159 and degree 2190 without any noticeable flaw. Although some numerical degradation near the poles could be expected, we found no significant degradation up to $\pm 89.99999^\circ$ latitude. Also sample cases were used as tests for accuracy, performance and reliability of our geopotential algorithm for integrating Earth orbits.

The other major gravitational perturbations taken into account were those due to the Sun and the Moon, whose gravitational potentials can be represented by point-mass models. The acceleration due to a point-mass is modeled by the usual Newtonian expression

$$\ddot{\mathbf{r}}_{Sun,Moon} = \mu_p \left(\frac{\mathbf{r}_p - \mathbf{r}}{|\mathbf{r}_p - \mathbf{r}|^3} - \frac{\mathbf{r}_p}{|\mathbf{r}_p|^3} \right), \tag{A12}$$

where μ_p is the gravitational coefficient (GM_p) of the perturbing body, and \mathbf{r}_p is the inertial position vector of the perturbing body. Note that the inertial coordinates of the Sun and the Moon are obtained analytically, and are characterized by an accuracy of 10^{-3} degrees for the Sun and 10^{-2} degrees for the Moon. For the numerical integration of the orbit the predictor-corrector algorithm ODE [24] with variable order and step-size was used to tolerances set around 10^{-12} . The set of first order differential equations for position, \mathbf{r} , and velocity, \mathbf{v} , were integrated in the J2000 inertial coordinate system, and they are given by the following expressions

$$\begin{aligned}
\dot{\mathbf{r}} &= \mathbf{v}, \\
\dot{\mathbf{v}} &= \mathbf{a}_g + \mathbf{a}_{Sun} + \mathbf{a}_{Moon},
\end{aligned}$$

where \mathbf{a}_g is the geopotential acceleration, and \mathbf{a}_{Sun} , \mathbf{a}_{Moon} are the corresponding perturbing gravitational accelerations due to the Sun and Moon respectively. Where needed, care was taken to compute the transformation between the J2000 inertial system and ITRF system

using the SOFA library [25].

- [1] Tinto, M., de Araujo, J.C.N., Aguiar, O.D., Alves, M.E.S. "Searching for gravitational waves with a geostationary interferometer." *Astroparticle Physics*, **48**, p. 50-60 (2013)
- [2] Thorne, K. S., In: *Three Hundred Years of Gravitation*, 330-458, Eds. Hawking, S. W., & Israel, W., (Cambridge University Press, New York) (1987)
- [3] Weber, J., "Observation of the Thermal Fluctuations of a Gravitational-Wave Detector", *Phys. Rev. Lett.*, **17**, (1966) 1228.
- [4] <http://www.ligo.caltech.edu/> .
- [5] <http://www.virgo.infn.it/> .
- [6] "LISA: Unveiling a hidden Universe", ESA publication # ESA/SRE(2011)3 (February 2011).
Also available at: <http://sci.esa.int/science-e/www/object/index.cfm?fobjectid=48364>
- [7] Ni, W. T., "ASTROD-An Overview", *Int. J. Mod. Phys. D*, **11** (7), 947 (2002)
- [8] Seto, N., Kawamura, S., & Nakamura, T., "Possibility of Direct Measurement of the Acceleration of the Universe Using 0.1 Hz Band Laser Interferometer Gravitational Wave Antenna in Space, *Phys. Rev. Lett.*, **87**, 221103 (2001)
- [9] Hiscock, B., Hellings, R. W., "OMEGA: A Space Gravitational Wave MIDEX Mission", *Bull. Am. Astron. Soc.*, **29**, 1312 (1997)
- [10] <http://pcos.gsfc.nasa.gov/studies/gravitational-wave-mission.php/> .
- [11] NRC 2010, <http://www.nap.edu/catalog/12951.html>
- [12] NASA solicitation # NNH11ZDA019L titled: *Concepts for the NASA Gravitational-Wave Mission*. Document available at: <http://nspires.nasaprs.com/external/> .
- [13] Tinto, M., & Alves, M. E. S., "LISA sensitivities to gravitational waves from relativistic metric theories of gravity" *Phys. Rev. D*, **82**, 122003 (2010)
- [14] Soop, E. M., *Handbook of Geostationary Orbits*, Kluwer Academic Publishers (Dordrecht, The Netherlands) (1994).
- [15] Tinto, M., & Dhurandhar, S. V., "Time-Delay Interferometry", *Living Rev. Relativity*, **8**, 4 (2005) <http://www.livingreviews.org/lrr-2005-4>
- [16] Barnes, J.A., *et al*, "Characterization of frequency stability", *IEEE Trans. Instrum. Meas.*, **IM-20** 105-120 (1977)

- [17] J.D. Prestage, M. Tu, S.K. Chung, and P. MacNeal, “Compact microwave mercury ion clock for space applications”. In: *Proceedings of the 39th Annual Precise Time and Time Interval (PTTI) Meeting*, November 27 - 29, 2007, Long Beach, CA (<http://www.ion.org/publications/browse.cfm?proceedingsID=68>)
- [18] Tinto, M., Estabrook, F. B., & J.A. Armstrong, 2002, “Time-delay interferometry for LISA”, *Phys. Rev. D*, **65**, 082003.
- [19] Pavlis, N.K., Holmes, S.A., Kenyon, S.C., Factor, J.K. “An Earth Gravitational Model to Degree 2160: EGM2008”, Presented at the 2008 General Assembly of the European Geosciences Union, Vienna, Austria, April 13-18 (2008)
- [20] Kuga, H. K., Carrara, V. “Fortran- and C-codes for higher order and degree geopotential and derivatives computation”, *Proceedings of XVI SBSR - Brazilian Symposium on Remote Sensing*, Iguassu Falls, Brazil, April 13-18, 2013, pp. 2201-2210 (2013) “www.dem.inpe.br/hkk/software/highgeopot.htm”
- [21] Baumgartel, L., “Whispering gallery mode resonators for frequency metrology applications”, Ph.D. Thesis, University of Southern California (2014)
- [22] Lemoine, F. G., Kenyon, S. C., Factor, J. K., Trimmer, R.G., Pavlis, N. K., Chinn, D. S., Cox, C. M., Klosko, S. M., Luthcke, S. B., Torrence, M. H., Wang, Y. M., Williamson, R. G., Pavlis, E. C., Rapp, R. H., Olson, T. R. “The Development of the Joint NASA GSFC and NIMA Geopotential Model EGM96”. NASA Goddard Space Flight Center, Greenbelt, Maryland, July 1998. NASA/TP-1998-206861 (1998)
- [23] Holmes, S.A., Featherstone, W.E. “A unified approach to the Clenshaw summation and the recursive computation of every degree and order normalised associated Legendre functions”, *Journal of Geodesy*, **76**, p. 279-299, (2002)
- [24] Shampine L. F., Gordon M. K. “Computer Solution of Ordinary Differential Equations” Free-man and Company, San Francisco, 1975.
- [25] IAU SOFA “IAU SOFA Software Collection”, last access December, 12, 2013 (www.iausofa.org)